Synthesis and characterization of β-SiC-ZrB₂ ceramic composites by spark plasma sintering

YONG-DEOK SHIN*, JIN-YOUNG JU, WON-SEOK CHO[a]

Department of Electrical Engineering, Wonkwang University, 344-2, Shin-Yong-Dong, IkSan, Chun Buck, 570-749, Korea.
[a]Department of Electrical Engineering, Hanbat National University, San 16-1, DuckMyung-Dong, Yuseong-Gu, DaeJeon, 305-719, Korea

The composites were fabricated by adding 0, 15, 30, 45vol.% zirconium diboride (hereafter, ZrB_2) powder as the second phase to silicon carbide (hereafter, SiC) matrix. The physical, mechanical, and thermal analysis and electrical properties of electroconductive SiC ceramic composites by spark plasma sintering(hereafter, SPS) were examined. Reactions between β-SiC and ZrB_2 were not observed in the XRD analysis. The relative density of mono SiC(hereafter, SZ00), SiC+15vol.% ZrB_2 (hereafter, SZ15), SiC+30vol.% ZrB_2(hereafter, SZ30) and SiC+45vol.% ZrB_2(hereafter, SZ45) composites are 90.93, 74.62, 88.64 and 88.12%, respectively. The XRD phase analysis of the electroconductive SiC ceramic composite reveals high of SiC and ZrB_2 and low of ZrO_2 phase. The lowest flexural strength, 108.79MPa, shown in SZ15 composite and the highest - 205.96MPa - shown in SZ00 without ZrB_2 powder at room temperature. The trend of the mechanical properties of the electroconductive SiC ceramic composites moves in accord with that of the relative density. The electrical resistivities of SZ00, SZ15, SZ30 and SZ45 composites are 4.57×10^{-1}, 2.13×10^{-1}, 6.74×10^{-4} and $4.95\times10^{-3}\Omega\cdot$cm at room temperature, respectively. The electrical resistivities of SZ00 and SZ15 have negative temperature coefficient resistances(hereafter, NTCR) in the temperature range from 25 to 100℃. The electrical resistivities of SZ30 and SZ45 have positive temperature coefficient resistances(hereafter, PTCR) in the temperature range from 25 to 100℃. The declination of V-I characteristics of SZ30 and SZ45 composites are respectively 4.5×10^{-3} and 3.5×10^{-2}. The rising temperature of SZ45 measured by the thermal image analyzer is 7.44℃ higher than SZ30 composite's. It is convinced that SZ30 composite by SPS can be applied for heater or electrode.

1. Introduction

SiC, which has the high melting point of 2,800℃ and the low thermal expansion coefficient of about 4.36×10^{-6}/℃ at 20-1000℃, is a thermochemistrical stable IV-IV-compound semiconductor; its heating-conductivity, thermal impact resistance, strength, and oxidation-resistance are excellent[1]. However, its sintering density cannot be obtained without sinter additives since it has the low diffusion coefficient caused by the strong covalent bond between Si and C. In addition, Under 1000℃, its electrical resistivity is considered as its NTCR; the electrical current cannot be restrained as the temperature rises, hence, overheating takes place[2].

ZrB_2, a transition metal boride, generally, has the high melting point of 3.200℃, high hardness, metal-like electric conduction, and high corrosion resistance against molded iron and slag; on the contrary, its level of intensity and oxidation resistance will be questioned when over 1,000℃ heated electric conductions are employed[3].

SiC and ZrB_2 can be compounded into SiC-ZrB_2 composite, one of the most promising candidate material, as the high and low electric conduction material and electrode; its essential features such as high electrical conductivity, superior oxidation resistance, and mechanical strength can be recognized in SiC-ZrB_2 composite[4-6]. In other word, each of atom's unique superior characteristics will be entirely preserved in SiC-ZrB_2 composite.

SiC ceramic can be obtained by hot press (hereafter, HP), one of the solid-state sintering process, between about 1,950 ~ 2,100℃. To lower HP's temperature below 1950℃, liquid-phase forming additives such as $Al_2O_3+Y_2O_3$ are applied frequently nowadays[7]. Easier activation due to the better clarity of the particle's surface, high speed diffusion, highly efficient heating, faster sintering transformation, supply of high energy density can be found in SPS, not HP; therefore, it can be easier to obtain a high quality sintered compact at lower temperature and quicker. When it comes to various sintered compact such as metal and ceramic, it is possible to sinter them in the wide range of temperature and pressure and easy to control sintering microstructure which has no grain growth. Although SPS is similar to HP, there are differences; electric field is applied into up-bottom electrode as well as powders directly in SPS[8-11].

However, according to many reports on the processing parameters for new material preparation, the mechanisms for densification of sintered compacts are yet unclear, and systematic examinations on the mechanisms unveiling SPS features have a long way to go[12-15].

In this work, we applied SPS for quick sintering at 1,500℃, 450~600℃ lower than HP's, to attain SiC-ZrB$_2$ composite which is the high density sintered compact. We examined XRD, relative density, SEM, EDS, thermal image, V-1 Characteristic, and electrical resistivity of SiC-ZrB$_2$ composite, acquired through SPS, to analyze its mechanical and electrical properties. We discussed densification and electrical conduction mechanisms, thus, if SiC-ZrB$_2$ composite can be used as an energy friendly ceramic heater or electrode.

2. Experimental Procedure

2.1. Compact Sintering

In this study, high-pure β-SiC(H. C. Starck, Germany, Grade BF12) and ZrB$_2$(H. C. Starck, Germany, Grade B) were used as starting powders. The powder mixture of β-SiC+0vol.%ZrB$_2$ will be named as (SZ00), 15vol.%ZrB$_2$ (SZ15), 30vol.%ZrB$_2$ (SZ30) and 45vol.%ZrB$_2$ (SZ45); ZrB$_2$ was used as the second phase.

A 120mmΦ diameter and 140mmL height polyurethane jar (volume: 1583.4㎖), contains acetone, a high purity SiC ball of diameter 10㎜Φ, 20㎜Φ(1:5 wt%) and different β-SiC+ZrB$_2$s, was planetary-ball-milled for 24 hours.

We dehydrate what we get from planetary-ball-milled process for 12 hours at 100℃, then, sieved dehydrated powders through a 60 mesh screen, respectively.

2.2 SPS Process

We enclosed the inside wall of 15mmφ inner diameter graphite die with a graphite foil and filled it up with the dried powder. Then, we employed the Dr. Sinter SPS-515S apparatus (Sumitomo Coal Mining Co.Ltd., Tokyo, Japan) in order to sinter the powder under following conditions: 1,500℃, 10Pa vacuum, and uniaxial pressure of 30MPa.

The following sintering parameters were used: (i) raising its temperature by 100℃/min from room to 1,500℃ and holding it for 5 minutes at the highest temperature; (ii) constant pressure of 30MPa were lasted for the entire examination; and (iii) on/off pulse sequence is 12:2(one pulse time: 2.78ms). After 5 minutes, the pressure was released, and the electrical current was shut off. The final SiC-ZrB$_2$ composites were as big as approximately 15mmΦ in diameter and 5mmL in thickness.

2.3 Characterization Techniques

Relative densities of the final SiC-ZrB$_2$ composites

were measured 10 times per each composite by the Archimedes method and the theoretical densities were calculated according to the rule of mixture(3.217g/㎤ for β-SiC, 6.085g/㎤ for ZrB$_2$). Phase identifications and EDS - a member of SEM - analysis of the sintered compacts were analyzed by XRD (D-Max 220V Rigaku, Japan) with CuKα radiation.

The final SiC-ZrB$_2$ composites were ground by a diamond wheel, and the disks were machined to produce 1.0×0.7×10mm^3 dimension bars approximately. Then, the tensile surfaces of the bars were polished by using 1μm diamond paste and were beveled at 45 degree for mechanical testing(ASTM F394-78). Three-point flexural strength was measured at room temperature with outer and inner spans of 10mm and 8mm, 5 times per each sintered compact, respectively (Instron, Model 4204, USA). After that, the microstructure of the fractured surface was observed by SEM (XL30S Phillips, USA).

The two of machined pieces -SZ30 and SZ45- were cut by using wire-EDM (Electrical Discharge Machining) to measure each piece's electrical resistivity. The electrical resistivity of each machined piece was measured through Pauw method from 25℃ to 100℃ by 250 times[16]. The other two pieces -SZ00 and SSZ15- were cut by NC-lathe machine and their electrical resistivities were measured through 3-point probe method. The thermal images of SZ30 and SZ45 were analyzed by a thermal image camera(TVS-100E, Avio, Japan).

3. Results and discussion

3.1 Relative density

As Fig. 1 demonstrates, the relative densities of SZ00, SZ15, SZ30, and SZ45 are 90.93, 74.62, 88.64, 88.12% respectively, when the amount of ZrB$_2$ increases by 15vol.% from 0 to 45, the porosity changes 9.07 ➔ 25.38 ➔ 11.36 ➔ 11.88%; the porosity of SZ15 is the highest one, and SZ00 has the lowest one.
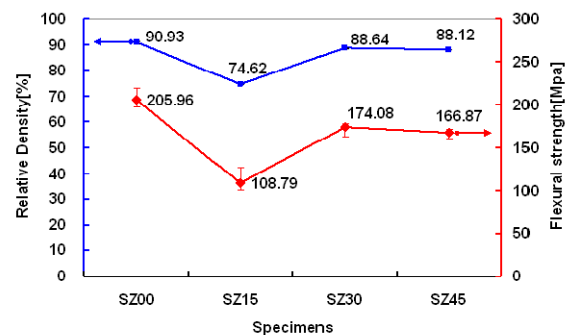
Fig. 1 Relative density and three-point flexural strength.

Amorphous glass is formed on the surface because of the sintering caused by discharge and the reaction equation

of (1)[17] and (2)[18] since SiO$_2$ is always contained in SiC; it is considered that the amorphous glass has the biggest oxidation resistance effect. That is why the relative density of SiC single crystal is the highest one.

In Table 1, by the reaction equation (1)[17], the volume variation of SZ15 rises by 53.58% as the weight variation of SZ15 increases by 14.5934%; this may explain why its relative density is the lowest one.

Table. 1 Mass and volume variation of the SiC-ZrB$_2$ composites

Specimen	Weight before sintering[g]	Weight after sintering[g]	Weight variation[%]	Volume before sintering [cm^3]	Volume after sintering [cm^3]	Volume variation [%]
SZ00	2.8425	2.993	▲ 5.2946	0.8836	1.0232	▲ 15.80
SZ15	3.2227	3.693	▲ 14.5934	0.8836	1.3570	▲ 53.58
SZ30	3.6028	3.568	▼ 0.9659	0.8836	0.9872	▲ 11.72
SZ45	3.9829	3.956	▼ 0.6754	0.8836	0.9960	▲ 12.72

When SiC and ZrB$_2$ react with oxygen, oxygen reacted atoms produce ZrO$_2$ (s), SiO$_2$ (s,l), B$_2$O$_3$(l,g), SiO(g), CO(g), and CO$_2$ (g); we can see some part of or whole of them are appeared in the reaction equation (1) through (5) [17-18].

$$ZrB_2 + SiC + 4O_2(g) \rightarrow ZrO_2(s) + B_2O_3(g) + SiO_2(g) + CO(g)$$
(1)

$$SiC + \frac{3}{2}O_2 = SiO_2(s,l) + CO(g)$$
(2)

$$ZrB_2 + \frac{5}{2}O_2 = ZrO_2(s) + B_2O_3(l)$$
(3)

$$SiO_2 + CO = SiO(g) + CO_2(g)$$
(4)

$$B_2O_3(l) = B_2O_3(g)$$
(5)
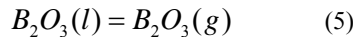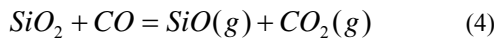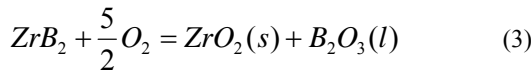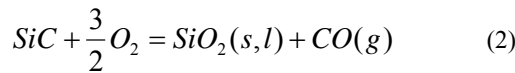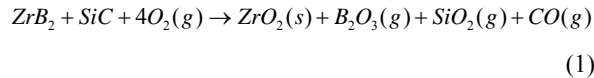
Like above, since condensed and vapor species are created, it is difficult to state the exact reaction speed of the measurement of mass change. In other word, weight gain and weight loss take place simultaneously[17]. The bigger difference in volume variation between SZ45 and SZ30 over in weight variation between them makes the relative density of SZ45 lower than SZ30's.

The SZ30 preference of producing condensed, vapor species, B$_2$O$_3$, and SiO$_2$ is greater than SZ45 preference by the equation of (1) through (5), thus the SZ30 weight variation, 0.9659% has to higher than SZ45's, 0.6754%

As it is illustrated in Table 2, the amount of Si in SZ45, 37.42atom.% is higher than in SZ30, 23.03atom.%. It is reported that the borosilicate glass layer, which have SiO$_2$ and B$_2$O$_3$, are formed on exposed surfaces and protect atoms from the inward diffusion of oxygen more effectively than condensed and vapor species of ZrO$_2$ phase, created according to the reaction equation (1) to (5)[18].

Moreover, it is demonstrated the amount of C in SZ15, 34.97atom.%, is smaller than in SZ30, 43.39atom.%; it can be interpreted that the formation of vapor species CO(g) by the reaction equation (1) through (5) is conspicuously observable.

Table. 2 EDS analysis of the SiC-ZrB$_2$ composites.

Specimen / atom	SZ00	SZ15	SZ30	SZ45	Remarks
Si	56.80	37.08	23.03	37.42	atom%
Zr	0.00	2.91	4.79	13.56	
B	0.00	14.31	19.62	25.43	
C	24.34	34.97	43.39	19.17	
O	18.87	10.74	9.17	4.42	
Total	100.00	100.00	100.00	100.00	

3.2 Phase analysis and microstructure

As demonstrated in Fig. 2, single crystal SZ00 only has SiC phase, however, XRD analysis of SiC-ZrB$_2$ composites - SZ15, SZ30, and SZ45- demonstrate that ZrO$_2$ phase is shown most frequently in SZ15. The reason is this; the borosilicate glass, rather than condensed and vapor species, is more likely produced in SZ45 than SZ30 by the reaction equation (1) through (5). By the reaction equation (1) ~ (5), ZrO$_2$ condensed and vapor species are mostly formed in SZ15, hence its relative density is the lowest; XRD analysis in Figure 2, pointing up ZrO$_2$ phase is mostly shown in SZ15, can supplement above explanation. In Table 2, as EDS analysis describes, the amount of Si should decreases since SZ45 has 15vol.% more ZrB$_2$ than SZ30 theoretically, nevertheless, SZ45 has more amount of Si than SZ30 by 14.39atom.%.

In addition, microstructure observation in Fig. 3 elucidate that the porosity of SZ00 - 9.07% is the lowest one, and SZ15 has the highest porosity, 25.38%. The porosity of SZ30 – 11.36% is lower then that of SZ45, 11.88%.

(a) SZ00

(b) SZ15

(c) SZ30

(d) SZ45
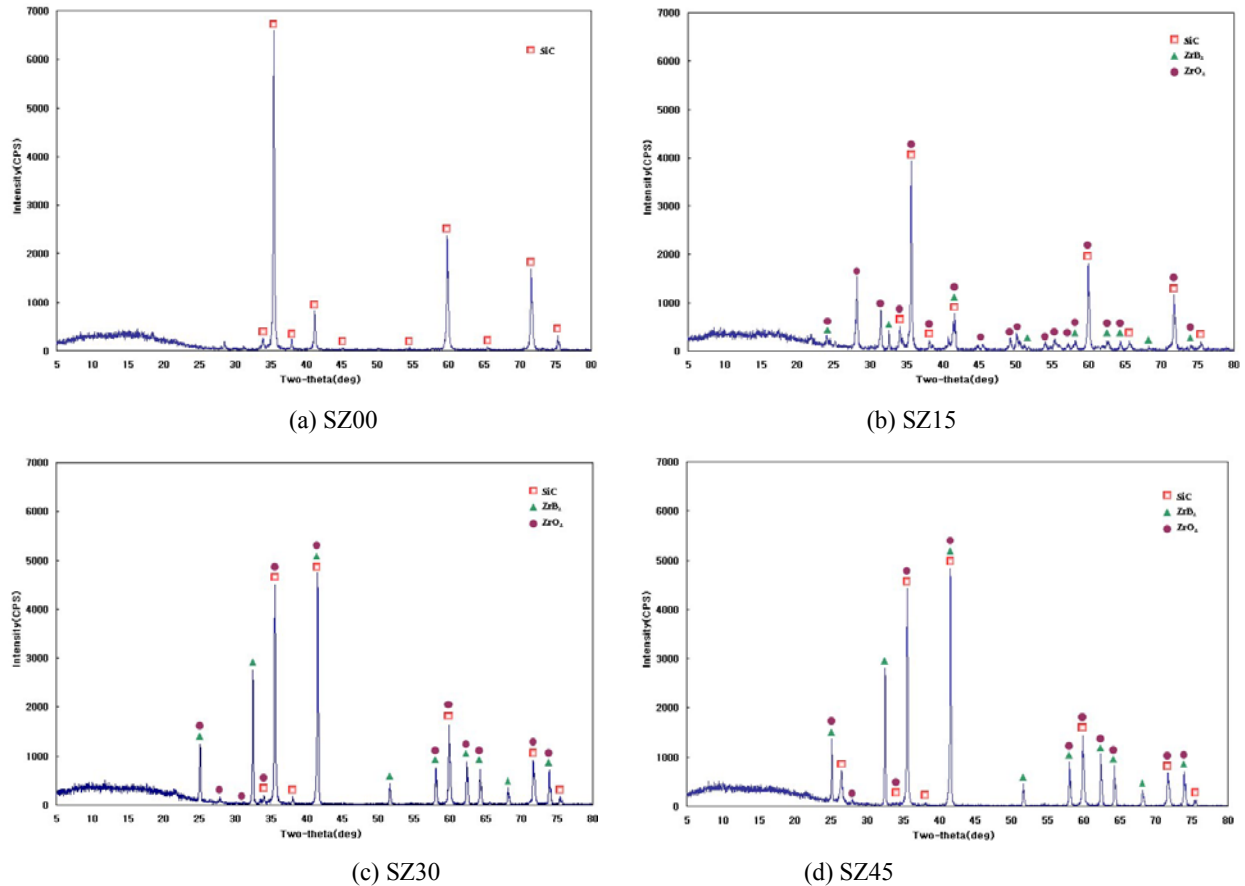
Fig. 2 X-ray diffraction analysis of the SiC-ZrB$_2$ composites

3.3 Mechanical properties

In Fig. 1, the flexural strengths of SiC-ZrB$_2$ composites place in between $100.11 \sim 219.55$MPa is lower than that of no porosity SiC and ZrB$_2$ single crystal, $350\sim500$MPa and $200\sim359$MPa respectively [19-22]. Generally, flexural strength has a positive relationship with grain growth of annealed ceramic. According to reports [23-25], as phase-shaped of ceramic microstructure become coarse due to ceramic annealing, fracture toughness of the ceramic increases and the level of flexural strength go down. When the second phase composition and annealing take place properly, it strengthens the microstructure of ceramic and avoids lowering the level of flexural strength.

In Fig. 1, the flexural strength of SZ00, SiC single phase, is 205.96MPa, when those of SiC ZrB$_2$ composites - SZ15, SZ30, and SZ45 - are 108.79, 174.08, and 166.87MPa, respectively. The reason why SZ15 flexural strength is lowest is following; SiC and ZrB$_2$ react with oxygen hence ZrO$_2$(s), SiO$_2$(s,l), B$_2$O$_3$(l,g), SiO(g), CO(g) and CO$_2$(g)[17] are generated in sintering process by (1) reaction equation, and the amount of porosity into which volatile component transferred in SZ15 is the biggest, 25.38%.

The flexural strength I obtained above, 108.79MPa, is too much lower compare to that of SiC-ZrB$_2$ composite SZ15 without porosity, $327.5\sim478.9$MPa, according to $\sigma_c = \upsilon_f \sigma_{SiC} + (1-\upsilon_f)\sigma_{ZrB_2}$; transformation of grain boundary and porosity can explain the reason why. Furthermore, the gained flexural strength of SZ30 and SZ45, 174.08 and 166.87MPa, are also lower compare to that of SZ30 and SZ45, $305\sim457.7$ and $282.5\sim436.6$MPa, having no porosity, respectively. The following equation, $\sigma = \sigma_0 \exp(-\kappa\alpha)$ (σ_o means zero defect flexural strength, α denotes residual porosity, and κ is constant), measures ceramic flexural strength and is well in accord with the equation above[26].

3.4 Electrical resistivity

The resistivity of SiC single crystal at room temperature is approximately 0.13Ω·cm; due to its NTCR characteristic, the resistivity drops to the point of 0.1Ω·cm when the temperature goes up to 250℃. In contrast, the resistivity goes up about 0.16Ω·cm when the temperature reaches around 900℃ because of its PTCR characteristic.

The resistivity of SiC polycrystalline is 0.1 to 0.3Ω·cm at room temperature. Its NTCR characteristic make resistivity go down by one-third under the temperature of 800℃, and it goes up over 800℃ due to its PTCR characteristic.
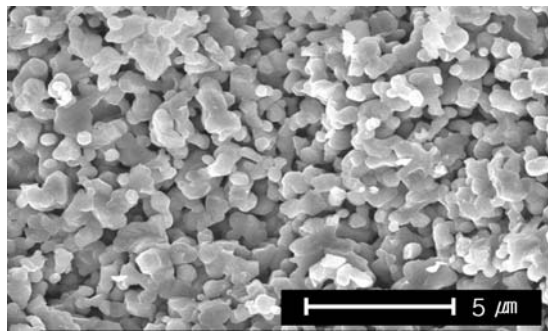
(a) SZ00
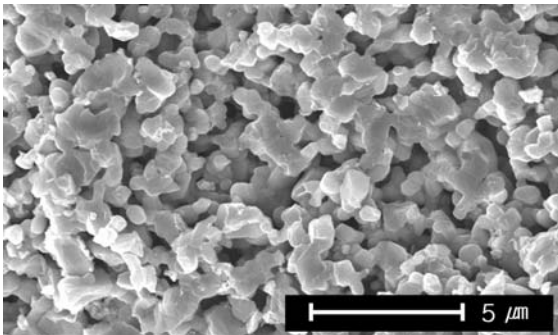
(b) SZ15
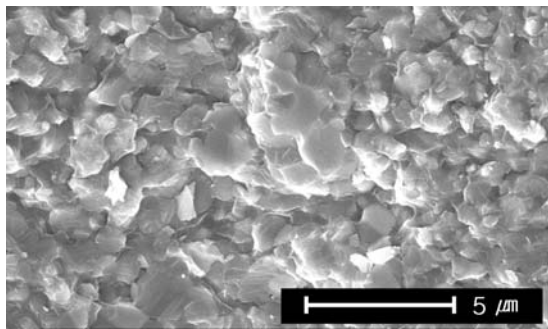
(c) SZ30
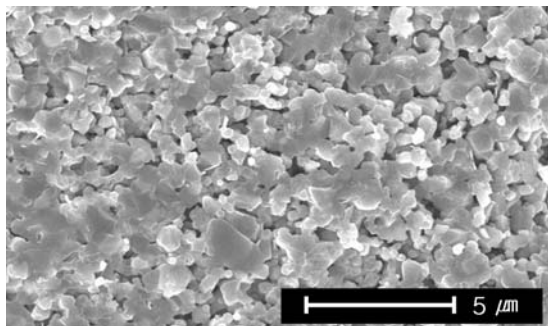
(d) SZ45

Fig. 3 SEM micrographs of the fracture surface.

The fact that grain of SiC polycrystalline is smaller and more amount of grain boundary than SiC single crystal makes above difference; grain in polycrystalline

grows as sintering temperature increases up to 800℃, hence its electric resistivity tends to go down[27].

The electrical conduction mechanism of SiC polycrystalline can be explained as the band model having potential barriers originated in grain boundaries. It is predominant that the conduction climbs over the barriers with the help of thermal excitation in high temperature ranges, and passes through the barriers in the form of tunnel and bulk in low temperature ranges [27].

In Fig. 4, it is shown that the electric resistivity of SiC-ZrB₂ composites - SZ00, SZ15, SZ30, and SZ45 - is 4.57×10^{-1}, 2.13×10^{-1}, 6.74×10^{-4}, 4.95×10^{-3} Ω·cm at room temperature, and 2.94×10^{-1}, 1.03×10^{-1}, 8.79×10^{-4}, 6.04×10^{-3} Ω·cm at 100℃, respectively. In addition, each composite's resistance temperature coefficient is -4.76×10^{-3}/℃, -6.89×10^{-3}/℃, 4.06×10^{-3}/℃, 2.94×10^{-3}/℃, in that order.

It is verified that SZ15 has NTCR characteristic since its resistance temperature coefficient is -6.89×10^{-3}/℃, which is illustrated in Figure 4 as well. The reason why SZ15 has NTCR characteristic is the chain formation of transition metal ZrB₂ grain is partially created; SiC electrical conduction mechanism, rather than grain boundary current, predominantly flows along with the created grain.
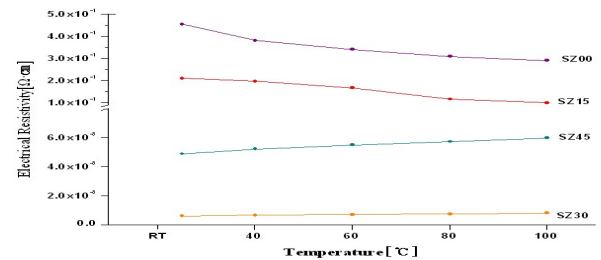
Fig. 4. Temperature dependence of electrical resistivity

SZ30 and SZ45 have PTCR characteristic because an electrical current flows predominantly by ZrB₂ grain - the second phase - chain formation which has low electrical resistivity. SZ45 electrical resistivity at room temperature and resistance temperature coefficient from room temperature to 100℃ is 7.34 times and 0.72 times bigger and smaller than SZ30's respectively. SZ30, having PTCR characteristic, has lower electrical resistivity, higher resistance temperature coefficient, and better mechanical properties than SZ45. I believe that SZ30 is more suitable than other composites to be applied for ceramic heater or electrode material of ohmic contact.

3.5 Characteristic and thermal image

As it is shown in Figure 5, the slope of V-I characteristic of SZ30 and SZ45 is 2.72×10^{-2} and 1.79×10^{-1} at room temperature and 3.42×10^{-2} and 2.19×10^{-1} at 100℃, respectively. The slope of SZ30 and SZ45 curves hardly get widened as temperature goes up, 4.5×10^{-3} and 3.5×10^{-2}; they have linearity hence, can be employed for the electrode material of ohmic contact.
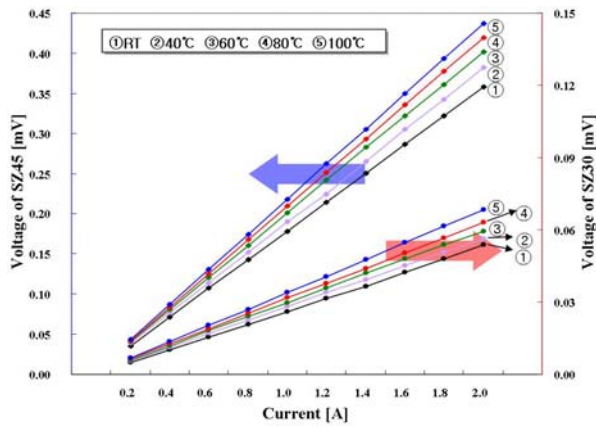
Fig. 5. V-I characteristic curves

3A applied into SZ30 and SZ45 at room temperature as shown in Figure 6; temperature measured at 5 different points after one minute later is demonstrated in Table 3. When it comes to SZ30, the deviation of temperature in measured temperature at 5 points is 0.99℃; on the other hand, there is no deviation difference in SZ45. After one minute, temperature at 5 points, in average, increases by 13.36℃ in SZ45 which is 7.44℃ higher than SZ30's; it is because the temperature dependence of electrical resistivity of SZ45 is higher than SZ30's, generally.

(a) SZ30 at start

(a) SZ30 after 60sec

(b) SZ45 at start

(b) SZ45 after 60sec
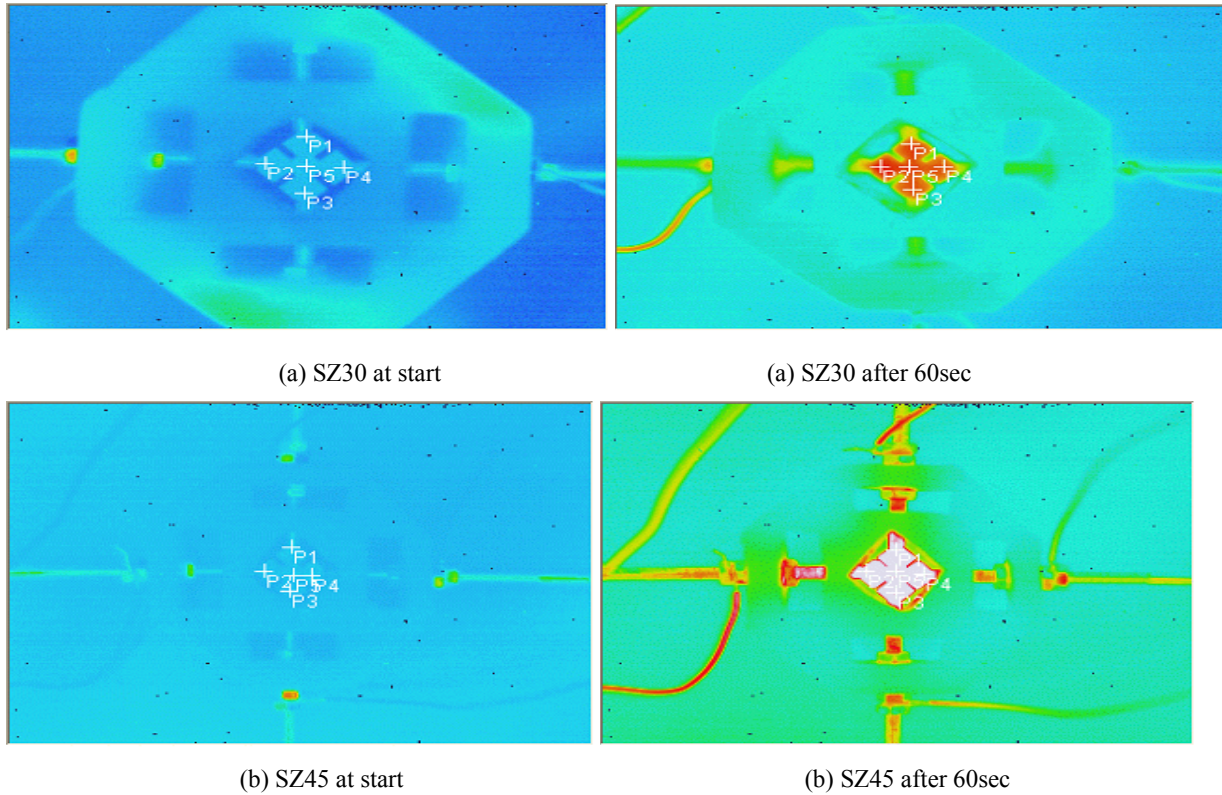
Fig. 6 Thermal image.

Table. 3 Point temperature of the SiC-ZrB$_2$ composites.

Specimen	SZ30		SZ45	
Time (sec) point[℃]	Start	60	Start	60
P1	23.70	29.46	21.78	35.19
P2	23.70	30.27	21.87	35.19
P3	23.61	29.28	21.87	35.19
P4	23.70	29.28	21.87	35.19
P5	23.61	29.64	21.78	35.19

4. Conclusion

The characteristic of β-SiC and the three composites made of β-SiC and ZrB_2, increased by 15vol.% at each time, through SPS are followings:

1) The porosity SiC single crystal and the SiC-ZrB_2 composites are 9.07, 25.38, 11.36, 11.88%, and SiC single crystal has the highest relative density, 90.93% and SiC+15vol.%ZrB_2 composite has the lowest, 74.62%

2) There is no reaction between SiC and ZrB_2, but ZrB_2 exists in the form of the second phase.

3) The flexural strength of SiC single crystal and three SiC-ZrB_2 composites are vary almost similar to their relative densities, SiC+15vol.%ZrB_2 has the lowest, 108.79MPa, and SiC single crystal has the highest, 205.96MPa.

4) The electrical resistivity of SiC single crystal and three SiC-ZrB_2 composites are 4.57×10^{-1}, 2.13×10^{-1}, 6.74×10^{-4}, 4.95×10^{-3}Ω·cm at room temperature, and 2.94×10^{-1}, 1.03×10^{-1}, 8.79×10^{-4}, 6.04×10^{-3}Ω·cm at 100℃, respectively.

5) The resistance temperature coefficient of SiC single crystal and three SiC-ZrB_2 composites are -4.76×10^{-3}/℃, -6.89×10^{-3}/℃, 4.06×10^{-3}/℃, 2.94×10^{-3}/℃, respectively. SiC and SiC+15vol.%ZrB_2 composites have NTCR characteristic; on the contrary, SiC+30vol.%ZrB_2 and SiC+45vol.%ZrB_2 composites have PTCR characteristic.

6) The slope difference in V-I characteristic per unit of temperature among SiC+30vol.%ZrB_2 and SiC+45vol.%ZrB_2 is infinitesimal then have linear relationship; it can be used for the electrode material of ohmic contact.

7) The temperature increase at each unit of point of SiC+30vol.%ZrB_2 is 0.99℃ in average; however, the temperature of SiC+45vol.%ZrB_2 at each unit of point does not fluctuate at all. After one minute, the average temperature increase at each unit of point of SiC+45vol.%ZrB_2 is 13.36℃, which is higher as much as 7.44℃ than SiC+30vol.%ZrB_2.

I believe that the optimized SiC-ZrB_2 composite for energy friendly ceramic heater and electrode material of ohmic contact through SPS should have excellent material properties, PTCR characteristic, low electric resistivity, and high resistance temperature coefficient; which means, in so far, it is considered that SiC+30vol.%ZrB_2 is the best alternative given to us.

Acknowledgement

Reference

[1] Patricia A. Hoffman, M. S Thesis, Pennsylvania State University, 1992.

[2] Hideto Hashiguchi, Hisashi Kimugasa, J. Ceram. Soc. Japan **102**(2), 160 (1994).

[3] M. Nakamura, I. Shigematsu, K. Kanayama, Y. Hirai, J. Mater. Sci. **26**, 6078 (1991).

[4] Y. D. Shin, J. Y. Ju, Trans. KIEE, **55**C(11), 505 (2006).

[5] Y. D. Shin, J. Y. Ju, , Trans. KIEE, **55**C(9), 434 (2006).

[6] Y. D. Shin, J. Y. Ju, T. H. Ko, Trans. KIEE, **56**C(9), 1602 (2007).

[7] Y. D. Shin, J. Y. Ju, Trans. KIEE, **48**C(2), 93 (1998).

[8] Zhengren Huang, Zhijian Shen, Luwei Lin, Mats Nygren, Dongliang Jiang, J. Am. Ceram. Soc., **87**(1), 42 (2004).

[9] Lianjun Wang, Wan Jiang, Lidong Chen, Shengqiang Bai, J. Am. Ceram. Soc., **87**(6), 1157 (2004).

[10] Takeshi Yamamoto, Hidetoshi Kitaura, Yasuhiro Kodera, Takashi Ishii, Manshi Ohyanagi, Zuhair A. Munir, J. Am. Ceram. Soc., **87**(8), 1436 (2004).

[11] Carmen M. Carney, Tai-Il Mah, J. Am. Ceram. Soc., **91**(10), 3448 (2008).

[12] K. A. Khor, L. G. Yu, & S. H. Chan, X. J. Chen, Journal of the European Ceramic Society **23**, 1855 (2003).

[13] Xiaoyan Song, Xuemei Liu, Jiuxing Zhang, J. Am. Ceram. Soc., **89**(2), 494 (2006).

[14] Shu-Qi Guo, Toshiyuki Nishimura, Yutaka Kagawa, Jenn-Ming Yang, J. Am. Ceram. Soc. **91**(9), 2848 (2008).

[15] Zhijian Shen, Mats Johnsson, Zhe Zhao, Mats Nygren, J. Am. Ceram. Soc., **85**(8), 1921 (2002).

[16] L, J. van der Pauw, Philips Res. Repts. **13**, 1-9 (1958).

[17] Alireza Rezaie, William G. Fahrenholtz, Gregory E. Hilmas, J. Am. Ceram. Soc., **89**(10), 3240 (2006).

[18] F. Monteverde, A. Bellosi, Journal of The Electrochemical Society., **150**(11), B552 (2003).

[19] Diletta. Sciti, Cesare. Melandri and Alida Bellosi, Adanced Engineering Materials, **6**(9), 775 (2004).

[20] Cathleen Mroz, J. Am. Ceram. Soc., Bull., **74**(6), 164 (1995).

[21] F. Monteverde, A. Bellosi,S. Guicciardi, Journal of the European Ceramic Society, **22**, 279 (2002).

[22] J. B. Hurst, S. Dutta, J. Am. Ceram. Soc. **70**(11), C303 (1987).

[23] M. Nader, F. Aldinger and M. J. Hoffmann, J. Mat. Sci. **34**, 1197 (1999).

[24] Y. W. Kim, M. Mitomo, H. Emoto, J. G. Lee, J. Am. Ceram. Soc., **81**(12), pp. 3136-3140, 1998.

[25] Y. W. Kim, M. Mitomo and H. Hirotsuru, J. Am. Ceram. Soc., **80**(1), 99 (1997).

[26] Weimin Wang, Zhengyi Fu, Hao Wang and Runzhang Yuan, Journal of the European Ceramic Society **22**, 1045 (2002).

[27] Akira Kondo, Journal of the Ceramic Society of Japan. Int. Edition, **100**, 1204 (1993).

*Corresponding author: ydshin@wonkwang.ac.kr